EPJ Photovoltaics **13**, 14 (2022)
© A. Fischer et al., Published by EDP Sciences, 2022
https://doi.org/10.1051/epjpv/2022009

EPJ Photovoltaics

Available online at:
www.epj-pv.org

Regular Article

Open Access

Impact of handling defects towards SHJ cell parameters

Andreas Fischer[*], Ioan Voicu Vulcanean, Sebastian Pingel, Anamaria Moldovan, and Jochen Rentsch

Fraunhofer Institute for Solar Energy Systems (F-ISE), Freiburg, Germany

Received: 30 June 2021 / Received in final form: 25 February 2022 / Accepted: 28 March 2022

Abstract. Within this paper, a systematic approach will be presented to specify the influence of defects caused by vacuum grippers onto silicon heterojunction solar cell parameters. The study focuses on the comparison between handling-induced defects originating from handling on the emitter or non-emitter side, and the comparison of handling-induced defects originating from handling before and after plasma enhanced chemical vapor deposition. The analysis was carried out by means of J–V measurements on manufactured silicon heterojunction solar cells and by means of suns photoluminescence imaging measurements on solar cell precursors. It is shown that local insufficient passivated regions caused by handling before passivation not only cause a local electrical defect at the point of handling, but also affect a large area around the insufficient passivated region. This had a significant negative effect on fill factor, short-circuit current, open circuit voltage and efficiency, which was found to be more severe for wafers handled on the non-emitter side.

Keywords: SHJ / handling / passivation defects

1 Introduction

In the photovoltaic industry, it was clear at an early stage that a high degree of automation is essential to ensure quality in mass production and to minimize costs [1,2]. Since the handling of fragile components with sensitive or functional surfaces is a major challenge [3], automated handling and the associated gripping technology are particularly affected here [4]. Gentle transport at very high speed [5] has been described as the biggest challenge in wafer handling in photovoltaic mass production. To remain competitive in terms of throughput, at least one substrate per second must be picked up, transported, and well aligned and positioned, while yield losses of less than 1% must be achieved [6]. The decisive criteria for the selection of handling components were thus assigned to the influence on process stability and damage minimization. With this basis, the focus of research was on the evaluation of handling systems with respect to induced mechanical loads and resulting breakage rates of silicon wafers [7,8]. For very surface sensitive cell concepts such as silicon heterojunction (SHJ), the requirements for the purity and nature of the silicon surface, which later becomes the interface between the silicon base substrate and the passivation layer, are now increasing. As a starting point, a clean, defect-free and specifically H-terminated silicon surface is required prior to passivation [9]. To meet these interface requirements, a new challenge is added in handling photovoltaic substrates: the handling system, which mainly consists of vacuum or Bernoulli grippers and conveyor belts, must not interfere with the sensitive, cleaned, possibly heated wafer surface. It is therefore necessary to thoroughly analyze handled wafers between process steps to identify defects caused by handling actions, to localize their cause and to estimate the resulting efficiency losses. In [10,11] it is described that amorphous silicon (a-Si) passivation defects resulting from grippers are mainly caused by particle transfer. This particle transfer leads to a characteristic imprint on assigned photoluminescence (PL) images. A reduction of transferred particles reduced or even removed these imprints in PL images and therefore the assigned losses in minority carrier lifetimes. With this reduced lifetime, due to particle contamination, it was concluded that recombination currents occur, and the overall passivation level will be lowered, resulting in a reduced cell efficiency. A similar observation was seen in [12], where cleaning of conveyor belts and grippers for the handling of wafers before passivation resulted in an efficiency gain of about 0.15% absolute. In [13] the impact of local surface defectivity on the SHJ solar cell performances were investigated. A strong effect on the efficiency, amounting to $-6\%_{rel}$ for ‘only’ 0.2% of the surface being defective, mostly driven by an FF loss, was shown. In this context the influence of defects, caused by particle transfer originating from vacuum grippers, onto SHJ cell parameters are investigated. The focus is on the comparison between handling-induced defects originating

[*] e-mail: andreas.fischer@ise.fraunhofer.de

This is an Open Access article distributed under the terms of the Creative Commons Attribution License (https://creativecommons.org/licenses/by/4.0), which permits unrestricted use, distribution, and reproduction in any medium, provided the original work is properly cited.

Experiment 1		Experiment 2	
M2 n-type Cz Si-Wafer			
Saw-damage etch + alkaline texturing			
Cleaning + HF-Dip			
Grasping at FS		Grasping at FS	Grasping at RS
PECVD a-Si(i) + a-Si(p) deposition at front side (FS)			
PECVD a-Si(i) + a-Si(n) deposition at rear side (RS)			
	Grasping at FS		
PVD TCO FS + RS			
Suns-PL-Imaging			
Metallization			
J-V-Measurement			

Fig. 1. Process flow of the experiment for the study of handling induced defects towards SHJ cell parameters. With wafers either grasped before and after a-Si deposition (Experiment 1) or grasped on the front side (FS) or rear side (RS) before a-Si deposition (Experiment 2).

from handling on the emitter or non-emitter side, and the comparison of handling-induced defects originating from handling before and after plasma enhanced chemical vapor deposition (PECVD).

2 Experimental details

The process flow of the experiments is shown in Figure 1. In experiment 1, textured and cleaned 180 μm thick, 1 Ωcm, n-type silicon Cz wafers were handled by vacuum grippers either before or after deposition of a-Si layer stacks by PECVD. In experiment 2, the handling was performed before deposition of the a-Si layer stacks, while the handling occurred either on the later emitter or non-emitter side. The handling was carried out on a test system built to evaluate various gripping devices (Fig. 2).

Within the test system, a wafer can be automatically gripped with a defined air pressure. To avoid scratches or particles from a substrate, the wafer is gripped from a frame where only the substrate edges are in contact with. The grasping is performed by four suction cups made of polyurethane, where a reproducible number of particles is transferred to the wafer surface. Following the handling action, the subsequent process steps were performed equally for both experiments. After deposition of the a-Si layer stacks, the wafers were coated on both sides with a 105 nm thick transparent conductive oxide (TCO) by physical vapor deposition (PVD) and were metallized afterwards. The analysis of the wafers was done by *J–V* measurements on the final processed SHJ cells and by suns photoluminescence imaging (SunsPLI) [14] on solar cell precursors before metallization. The *J–V* characteristics of the SHJ cells were evaluated using a solar simulator under AM1.5 and 100 mWcm^{-2} illumination. For the SunsPLI measurement, implied open circuit voltage (iV$_{OC}$) calibrated PL images were generated at illumination intensities between 0.005 and 1.5 suns. For each illumination intensity a respective pseudo current density (I_{suns}) was

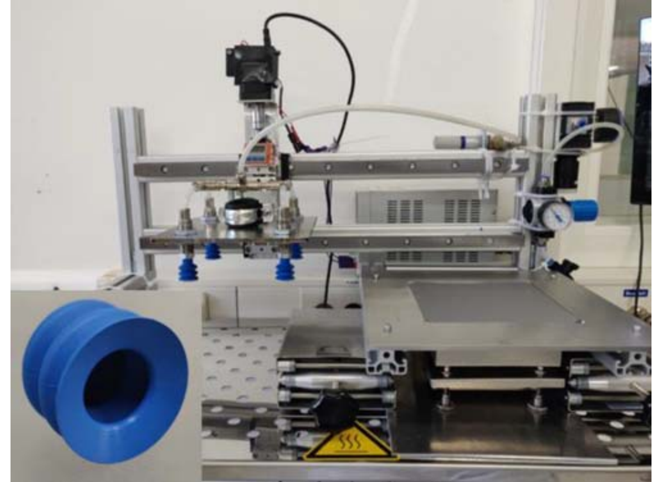

Fig. 2. Picture of tool used to grasp the wafers with magnified picture of one out of four suction cups used to grasp.

calculated by $I_{suns} = I_{SC} * (1 - suns)$, while the short-circuit current density (I_{SC}) value was obtained by *J–V* measurements of the finished cells. Each of these calculated I_{suns} values were multiplied with the data points (pixels) of the iV_{OC} image obtained at the corresponding illumination intensity, resulting in a power image. The power image consisting of pixels with the highest average power value was further used as image at maximum power ($P_{MPP, SunsPLI}$). To obtain a pseudo fill factor (pFF) image each of its pixels was calculated by the equation (1) below.

$$pFF(x, y) = \frac{P_{\mathrm{MPP,SunsPLI}}(x, y)}{iV_{OC,1Sun}(x, y) * \mathrm{I}_{SC}} \quad (1)$$

In the next step the pixels of pseudo efficiency images (η_{pseudo}) were calculated with the following equation (2).

$$\eta_{\mathrm{pseudo}}(x, y) = \frac{pFF(x, y) * I_{SC} * iV_{OC,1Sun}(x, y)}{P_{in}} \quad (2)$$

Unless otherwise indicated, the abbreviation iV$_{OC}$ will be used in the remainder of the text to refer to iV$_{OC}$ measured at one sun. It should be noted that the assumption of an average I_{SC} and I_{suns} used for all pixels does not correspond to reality. At a minimum value for defective areas, a lower loss in the iV$_{OC}$ at the MPP than in the iV$_{oc}$ is measured. Given averaged I_{suns} and I_{SC} values for the pFF calculation for all pixels, an overestimation of the pFF values will occur at these points.

3 Results and discussion

3.1 Comparison of handling before and after a-Si deposition

In this section the electrical effects of particle agglomeration on the wafer surface before and after deposition of the a-Si layer stack are investigated. Figure 3 shows an average image of eight iV$_{OC}$ calibrated PL images of wafers handled

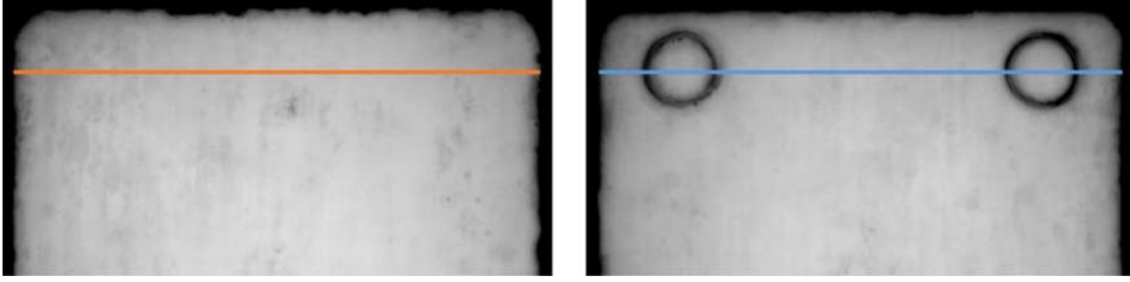

Fig. 3. Averaged iV_{OC} calibrated PL images of wafers handled before (left) and after a-Si deposition (right). With lines as guide to the eye for the following line plots.

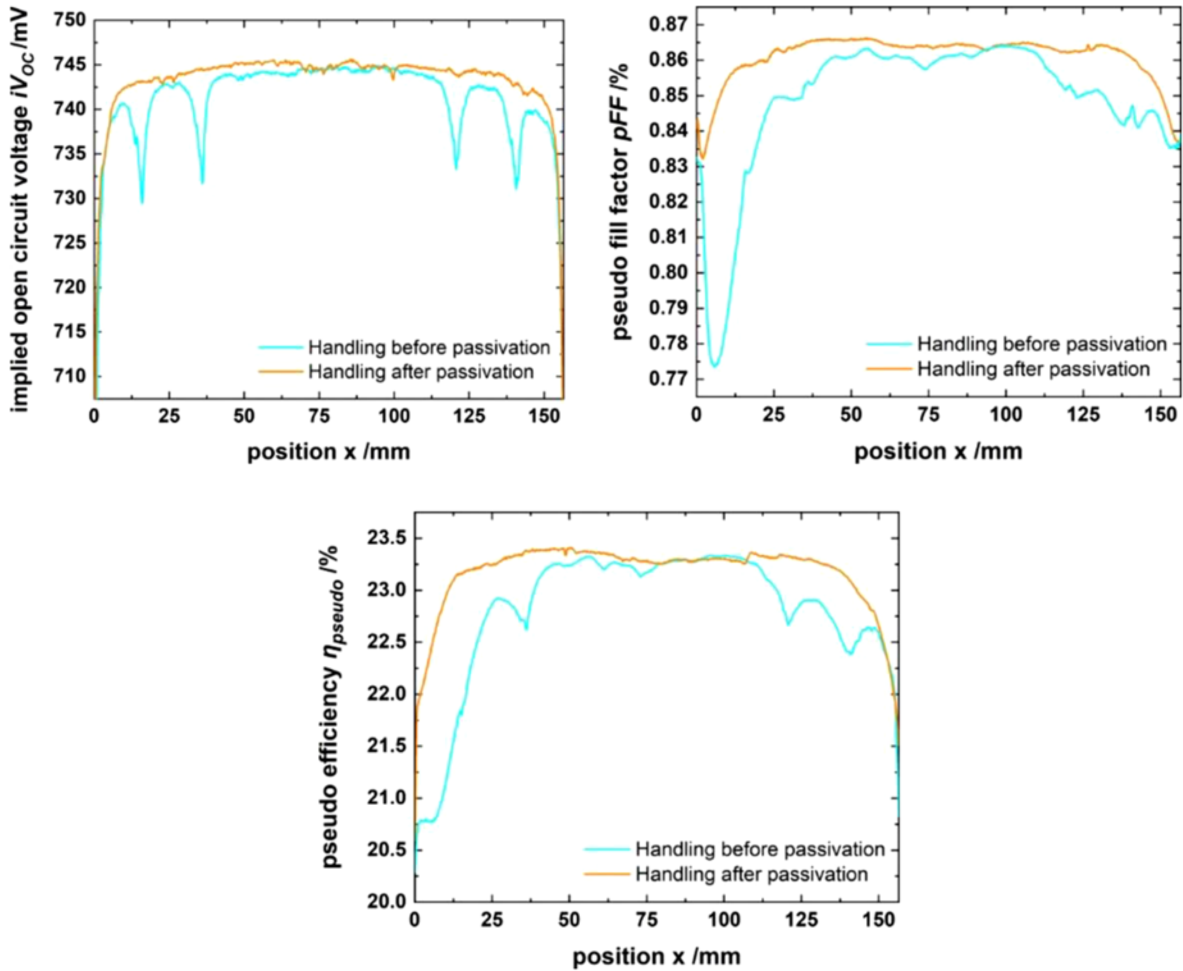

Fig. 4. Line plots of averaged images for η_{pseudo} (bottom), iV_{OC} (top left) and pFF (top right) handled before (blue) or after passivation (orange).

before and after a-Si deposition. While images of handled wafers after passivation do not show any characteristic electrical defects caused by handling, images of handled wafers before passivation show imprints of the used grippers.

The following graphs show line plots (Fig. 4) of averaged images for η_{pseudo}, iV_{OC} and pFF handled before or after passivation. The selected line of the line plots passes through the handling area of two suction cups and extends over the entire wafer width. For every line plot a lower value at the wafer edges is observed. This is due to passivation defects at the edges and a not optimized edge exclusion for the deposition of the TCO by PVD.

In the line plot of iV_{OC} calibrated averaged PL images of samples handled before and after a-Si deposition, the iV_{OC} increases sharply at the edges for about 5 mm and then changes only slightly towards the center of the wafer until a maximum is reached. For samples handled prior to

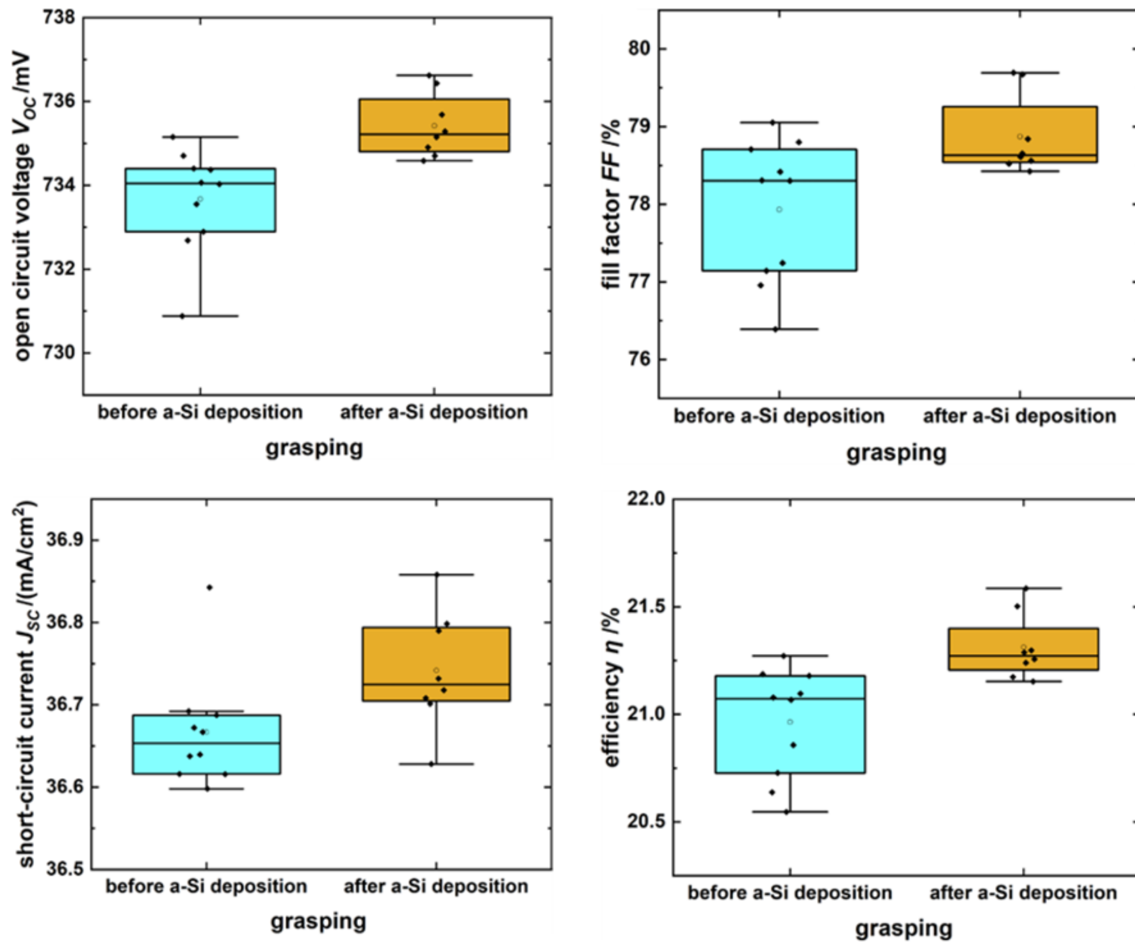

Fig. 5. Results for cell parameters of cells handled before or after passivation.

a-Si passivation, the slight increase in iV_{OC} towards the center is at the area of handling interrupted by sharp peaks to lower iV_{OC} values. Additionally, it can be seen, that the entire line plot of samples handled before passivation is shifted towards lower iV_{OC} values. The maximum iV_{OC} values of samples handled after passivation are not reached for samples handled before passivation.

In the line plots of pFF calculated averaged PL images of samples handled before and after a-Si deposition, it can again be seen that the pFF values increase from the edges towards the center of the wafer until a maximum is reached. This is more pronounced for samples handled after passivation, lasting 13 mm into the wafer middle. At the location of the maximum handling defect for the iV_{OC}, small peaks to higher values are now visible in the pFF. This is due to the pFF overestimation described in the previous chapter. Nevertheless, for samples handled before a-Si passivation, due to the resulting handling defects, a reduced pFF for about 50% of the wafer width compared to the value in the defect-free wafer center can be observed. The difference between these sharp defect peaks at the iV_{OC} and this smeared defect around the defect center for the pFF can be explained by the higher lifetimes at the iV_{OC} at the MPP. The higher lifetime corresponds to a higher diffusion length of the minority charge carriers, which causes a higher recombination probability at the local defect from a larger distance. As for the iV_{OC}, maximum pFF values of samples handled after passivation are not reached for samples handled before passivation.

The line plots of η_{pseudo} averaged calculated PL images of samples handled before and after a-Si deposition follow the trend of the line plots for pFF. The η_{pseudo} values increase from the edges in a similar way towards the wafer center. In the line plot for samples handled after passivation, a reduced η_{pseudo} due to edge defects can be seen from the wafer edges towards the wafer center for approximately 13 mm. For samples handled before a-Si passivation, a reduced η_{pseudo} value is observed for about 50% of the wafer width, compared to the values in the defect-free wafer center. This is assigned to resulting handling defects.

Based on this local analysis on solar cell precursors, a significant efficiency difference of solar cells handled before a-Si passivation and solar cells handled after a-Si passivation is expected. This difference should be driven by the fill factor, since the pFF influences a larger area than the iV_{OC} does. Although the solar cell precursors had an in-situ curing at the TCO deposition, the curing after metallization could have an additional positive annealing effect on small passivation defects. However, for the not passivated areas underneath the transferred particles an annealing effect is unexpected. Figure 5 shows the results of the cell parameters, measured by J–V-measurement.

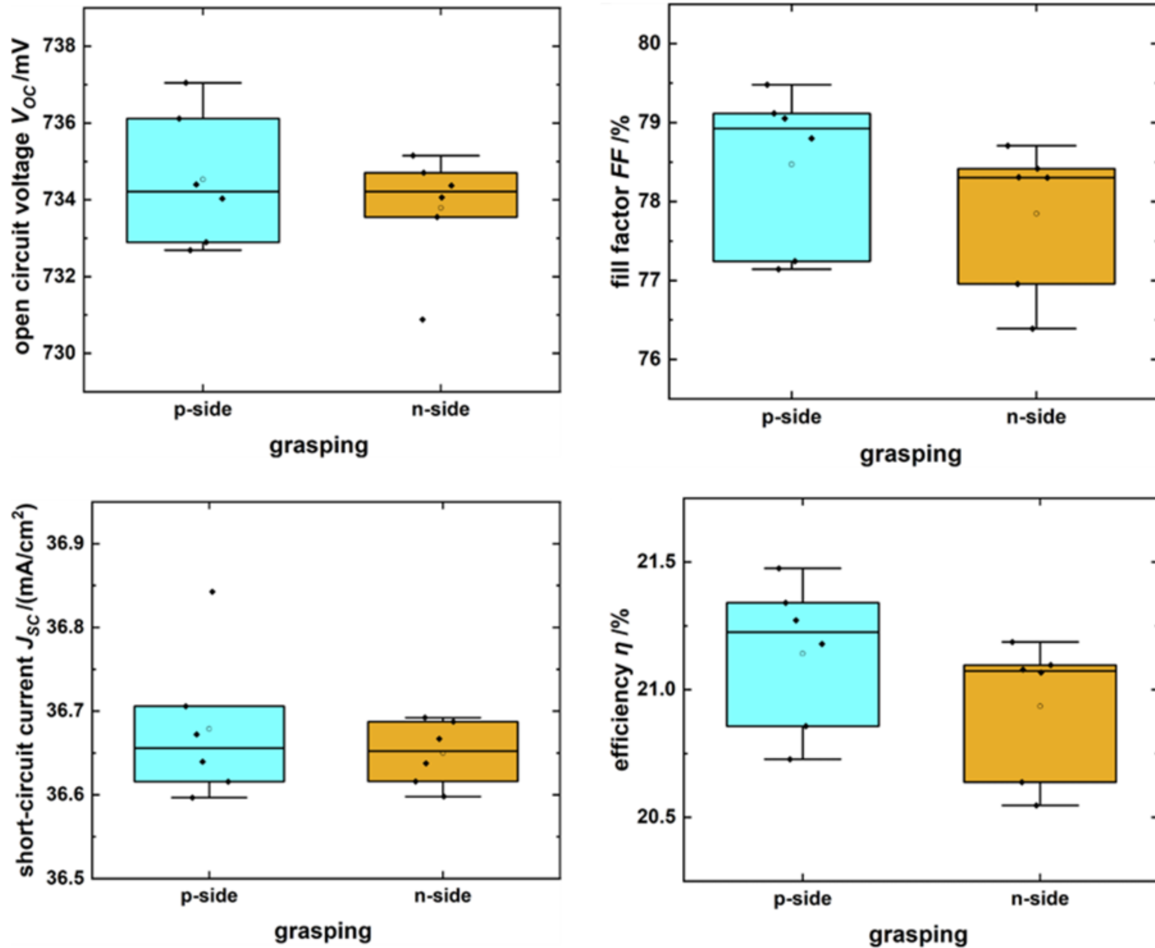

Fig. 6. Results for cell parameters of cells handled before passivation on the later emitter or non-emitter side.

For V_{OC}, the mean values are 733.7 mV and 735.4 mV for samples handled before and after passivation. The percentage loss is 0.24%. For FF, values of 77.93% for samples handled before and 78.87% for samples handled after a-Si deposition have been measured. Therefore, a percentage loss of 1.19% in the fill factor is calculated. The percentage difference of the mean values of the measured J_{SC} is 0.2% between samples handled before and after passivation. The mean values are 36.67 mA/cm^2 for samples handled before and 36.74 mA/cm^2 for samples handled after passivation. The percent losses of samples handled before passivation to samples handled after passivation in V_{OC}, FF and J_{SC} add up to a percent loss of 1.63% in η. The mean efficiencies are 20.96% for samples handled before passivation and 21.31% for samples handled after passivation. The losses due to handling before PECVD result in an absolute efficiency loss of 0.35%, measured by J–V measurements on SHJ solar cells. These results agree with literature and seem to be independent of the source of passivation defects. It holds true whether the defects are coming, like in our case, from particle transfer of grippers towards the wafer surface, defects applied by conveyor belts [12], wire sawing induced defects [15] or depassivation by scratches [13]. For all passivation defects efficiency losses are observed, which are mainly driven by losses in FF.

3.2 Comparison of samples handled on emitter side or non-emitter side

In this section the electrical effects of particle agglomeration on the emitter (p) side and non-emitter (n) side are analyzed. The difference of defects applied on the later emitter or non-emitter side can be seen in the cell results, which can be found in Figure 6.

For V_{OC}, the mean value is 734.5 mV for p-side handled samples and 733.8 mV for n-side handled samples. This results in a percentage difference of 0.1%. For FF, the higher mean values are also found for the samples handled on the emitter side. The percent difference is 0.8% and results from the mean value of 78.47% for samples handled on the p-side and the mean value of 77.85% for samples handled on the n-side. For the J_{SC}, the difference between samples handled on the p- or n-side is 0.08%. This is obtained by J_{SC} values of 36.68 mA/cm^2 for samples handled on the p-side and 36.65 mA/cm^2 for samples handled on the n-side. The percentage differences of samples handled on the emitter or non-emitter side for J_{SC}, V_{OC}, and FF add up to an efficiency difference of 0.98%. The average η values are 21.14% and 20.94% for samples handled on the p- and n-side, respectively. For both groups in this experiment a large overlap in the standard deviation for all cell parameters and especially the V_{OC} and J_{SC} can be

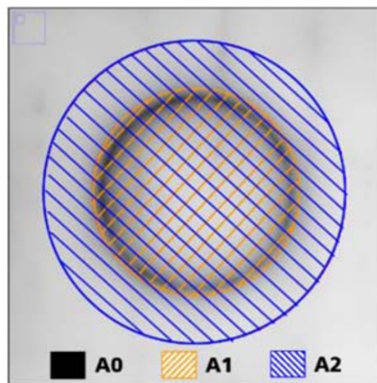

Fig. 7. Image section of a PL image of a wafer handled before passivation with marked different sized areas, used for the local loss analysis.

Table 1. Values for the different sized areas in Figure 12 and their percentage size fraction on a M2 wafer for one and four grippers.

	Area [mm^2]	M2 Wafer coverage (1 Suction cup) [%]	M2 Wafer coverage (4 Suction cups) [%]
A0	106.4	0.43	1.73
A1	368.8	1.50	6.00
A2	798.7	3.25	13.00

seen. In contrast to experiment 1, defects are always found in the handling area, which is not the case for samples handled after passivation. Therefore, other than gripper associated electrical defects contribute to a greater extent to the standard deviation of individual samples. Due to this fact it is necessary to perform local analyses, which is possible by the SunsPLI method for pseudo-cell parameters. Local loss analyses were performed using the measured iV_{OC} and calculated pFF and η_{pseudo} images. Figure 7 shows the different sized areas, used for the local loss analysis, while Table 1 shows their size, as well as their percentage size fraction on a M2 wafer for one and four grippers.

A0 describes the area of the dark ring of the visible defect and has an area of 106.4 mm^2. Area A1 has an area of 368.8 mm^2 and encloses area A0 and the area inside the circular defect. Area A1 has the same circular center as area A2 and has an area of 798.7 mm^2. The average iV_{OC}, pFF, and η_{pseudo} values of these areas were related to the location of the maximum η_{pseudo} of each sample. The results of the local loss analysis for handling on the *n* and *p* sides are shown in Figure 8.

Losses in iV_{OC} are higher for samples handled on the n-side than on the p-side. Handling on the p-side induces an iV_{OC} loss of 1.82% for A0, 1.24% for A1, and 1.04% for A2. Handling on the n-side has an iV_{OC} loss of 3.06% for A0, 1.7% for A1, and 1.32% for A2. One can observe that the difference of losses in iV_{OC} between the handling of the p- or n-side get smaller with increased area size. This can explain the small difference in the cells V_{OC} data of samples handled on the p- or n-side, seen in Figure 6. For the pFF, higher handling-induced losses are found for handling on the n-side. In this case the difference of losses in pFF does not decrease with increasing area size. The pFF loss values due to handling on the p-side are 2.05% for A0, 2.14% for A1, and 2.24% for A2. The handling on the n-side has pFF losses of 2.39% for A0, 2.92% for A1, and 2.82% for A2. One must mention, that with the assumption of constant I_{suns} and I_{SC} values for the pFF calculation possible shunting effects for wafers handled on the p-side are not considered. This could possibly lead to lower differences of pFF losses induced by handling on p- or n-side. Nevertheless, these results seem to confirm the trends in the FF data from Figure 6. The loss in η_{pseudo} for samples handled on the p- or n-side are calculated by adding the losses in iV_{OC} and the losses in pFF. Losses of η_{pseudo} are higher for handling on the n-side than for samples handled on the p-side for all areas measured. The η_{pseudo} loss of samples handled on the p-side (n-side) are 3.95% (5.43%) for A0, 3.35% (4.57%) for A1, and 3.25% (4.1%) for A2. The larger the considered area around the defect, the greater the proportion of losses due to pFF. Comparing this local analysis with the cell data in Figure 6, similar effects can be observed. The lower (pseudo-)efficiency for wafers handled on the n-side, compared to wafers handled on the p-side, is mainly driven by losses in (pseudo-)FF. J_{SC} and V_{OC} showed no significant impact on η, whether the handling was carried out on the p- or n-side. In the local analysis, the iV_{OC} losses due to handling on the n-side at the point of maximum defect also contributes to an increased loss of pseudo-efficiency at the point of maximum defect. However, this loss seems to be only local and becomes less and less as the examined area becomes larger. These results apply for defects resulting from particle transfer described in [10]. The transferred particles are in the range of 0.1 μm to 1.2 μm and have a surface coverage of approximately 1.6% at the handled area. For heavy damaged areas coming for

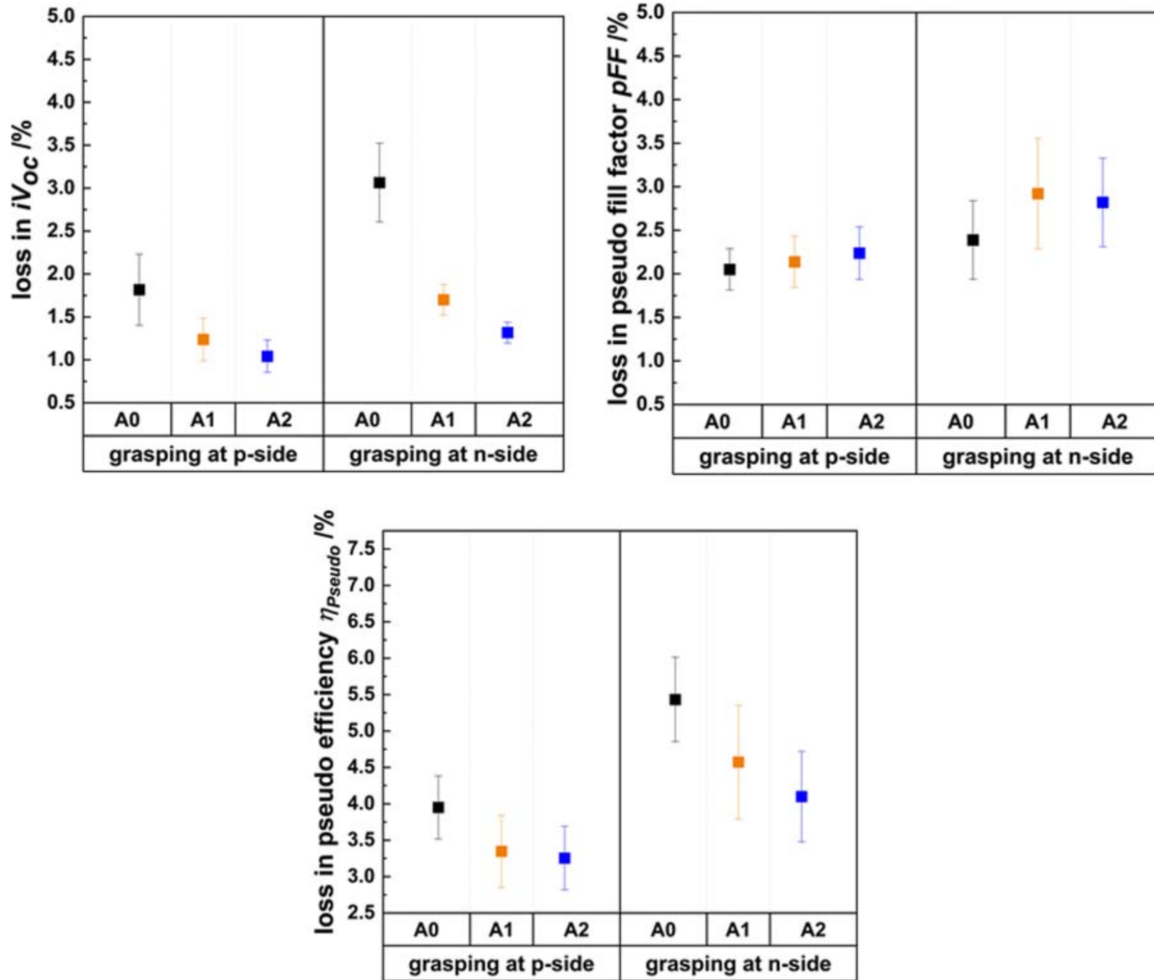

Fig. 8. Graphs showing the local loss analysis for iVoc, pFF, and η_{pseudo} of wafers handled either on the later emitter or non-emitter side.

example from scratches, as stated in [12], a different contribution of J_{SC} and FF to the overall η losses was reported.

4 Conclusion

In this work the influence of defects caused by particle transfer originating from vacuum grippers onto SHJ cell parameters were investigated. It is shown, that handling after cleaning and before passivation and the associated particle carryover has a significant effect on all solar cell parameters. No visible defect of handling after passivation has been seen in the assigned PL images. For all samples handled prior to PECVD and analyzed by SunsPLI, characteristic defects in the form of reduced iV_{OC}, pFF and η_{pseudo} have been found at the grasping areas of the handled wafers. It was presented that these defects not only cause a local defect at the point of handling, but also affect a large area around the maximum defect. For J–V measured SHJ cells it was shown that these defects caused a high η loss of 0.35% absolute, which is mainly driven by losses in fill factor. The relative efficiency loss due to handling before passivation consisted of 73% losses in FF, 15% losses in V_{OC} and 12% losses in J_{SC}. Furthermore, the influence of handling at the later emitter or non-emitter side was investigated. For defects originating from a particle transfer, a larger negative electrical effect was found due to handling on the non-emitter side of a SHJ solar cell, before deposition of the passivation stack. The negative electrical effect is mainly driven by losses in FF, while losses in J_{SC} and V_{OC} couldnt be indicated as significant. By applying a local analysis of obtained iV_{OC} and calculated pFF and η_{pseudo} images it is shown, that within an area of ~800 mm^2 around a handling defect, which with four grippers makes up 13% of the total wafer area, η_{pseudo} drops by up to 4.1% relative to the maximum η_{pseudo} value of the respective sample. With this local loss analysis, it was demonstrated that it is possible to compare defects from different processes as well as to estimate the efficiency reducing potential of a single defect. In summary, it can be concluded that the handling of SHJ cells and in particular the non-emitter side can have a significant influence on all cell parameters. The losses described can only be recognized through a detailed analysis, as otherwise a large part of the effect is not visible, as the overall level is strongly influenced. This does not only

apply to grippers, but also to all wafer contacts prior to a-Si deposition, for example automation or chemical carriers, conveyor belts, wafer flippers and tray carriers.

Part of this work was funded by German Federal Ministry for Economic Affairs and Energy under contract number 0324189B (ProSelect).

Author contribution statement

All authors contributed equally to the paper.

References

1. K. Reddig, Photovolt. Int. **4**, 18 (2009)
2. J.J. Haase, in Proceedings of the IEEE 4th World Conference on Photovoltaic Energy Conversion, Waikoloa (2006), p. 1256
3. M. Schilp, Ph.D. thesis, TU Munich, 2006
4. A. Grubba, Ph.D. thesis, University of Dortmund, 2002
5. T. Giesen et al., Assembly Autom. **33**, 334 (2013)
6. International Technology Roadmap for Photovoltaic (ITRPV), 3rd Edition (2012)
7. X.F. Brun et al., Solar Energy Mater. Solar Cells 93, 1238 (2009)
8. C. Fischmann, in Proceedings of the 27th Eur. Photovolt. Sol. Energy Conf. Exhib., Frankfurt, 2012, p. 1171
9. H. Angermann, Appl. Surf. Sci. **312**, 3 (2014)
10. A. Fischer et al., AIP Conf. Proc. **2147**, 050002 (2019)
11. A. Fischer et al., in Proceedings of the 36th Eur. Photovolt. Sol. Energy Conf. Exhib., Marseille, 2019
12. R. Varache et al., in Proceedings of the 37th Eur. Photovolt. Sol. Energy Conf. Exhib., Lisbon, 2020
13. V. Giglia et al., Prog. Photovolt. Res. Appl. **28**, 1333 (2020)
14. B. Michl et al., Prog. Photovolt: Res. Appl. **22**, 581 (2014)
15. O. Nos et al., Solar Energy Mater. Solar Cells **144**, 210 (2016)

Cite this article as: Andreas Fischer, Ioan Voicu Vulcanean, Sebastian Pingel, Anamaria Moldovan, Jochen Rentsch, Impact of handling defects towards SHJ cell parameters, EPJ Photovoltaics **13**, 14 (2022)